Complexation and Toxicity of Copper in Higher Plants. I. Characterization of Copper Accumulation, Speciation, and Toxicity in *Crassula helmsii* as a New Copper Accumulator[1][W][OA]

Hendrik Küpper*, Birgit Götz, Ana Mijovilovich, Frithjof C. Küpper, and Wolfram Meyer-Klaucke

Universität Konstanz, Mathematisch-Naturwissenschaftliche Sektion, Fachbereich Biologie, D–78457 Konstanz, Germany (H.K., B.G.); University of South Bohemia, Faculty of Biological Sciences and Institute of Physical Biology, CZ–370 05 České Budejovice, Czech Republic (H.K.); University of Utrecht, Department of Inorganic Chemistry and Catalysis, 3584 CA Utrecht, The Netherlands (A.M.); Scottish Association for Marine Science, Dunstaffnage Marine Laboratory, Oban, Argyll PA37 1QA, Scotland, United Kingdom (F.C.K.); and EMBL Outstation Hamburg, Deutsches Elekronen-Synchrotron, D–22603 Hamburg, Germany (W.M.-K.)

The amphibious water plant *Crassula helmsii* is an invasive copper (Cu)-tolerant neophyte in Europe. It now turned out to accumulate Cu up to more than 9,000 ppm in its shoots at 10 μM (=0.6 ppm) Cu^{2+} in the nutrient solution, indicating that it is a Cu hyperaccumulator. We investigated uptake, binding environment, and toxicity of Cu in this plant under emerged and submerged conditions. Extended x-ray absorption fine structure measurements on frozen-hydrated samples revealed that Cu was bound almost exclusively by oxygen ligands, likely organic acids, and not any sulfur ligands. Despite significant differences in photosynthesis biochemistry and biophysics between emerged and submerged plants, no differences in Cu ligands were found. While measurements of tissue pH confirmed the diurnal acid cycle typical for Crassulacean acid metabolism, $\Delta^{13}C$ measurements showed values typical for regular C3 photosynthesis. Cu-induced inhibition of photosynthesis mainly affected the photosystem II (PSII) reaction center, but with some unusual features. Most obviously, the degree of light saturation of electron transport increased during Cu stress, while maximal dark-adapted PSII quantum yield did not change and light-adapted quantum yield of PSII photochemistry decreased particularly in the first 50 s after onset of actinic irradiance. This combination of changes, which were strongest in submerged cultures, shows a decreasing number of functional reaction centers relative to the antenna in a system with high antenna connectivity. Nonphotochemical quenching, in contrast, was modified by Cu mainly in emerged cultures. Pigment concentrations in stressed plants strongly decreased, but no changes in their ratios occurred, indicating that cells either survived intact or died and bleached quickly.

Heavy metals such as cadmium (Cd), copper (Cu), manganese, nickel (Ni), and zinc (Zn) are well known to be essential microelements for the life of plants (for Cd, see Lane and Morel, 2000). On the other hand, elevated concentrations of these metals induce inhibition of various processes in plant metabolism (for review, see Prasad and Hagemeyer, 1999; Küpper and Kroneck, 2005). Cu can occur in very high concentrations that are detrimental or even lethal to most plants. It is widely used as a pesticide in agriculture, and field runoff may easily reach concentrations of several micromolar (Gallagher et al., 2001). Photosynthetic reactions, both photochemical and biochemical ones, belong to the most important sites of inhibition by many heavy metals and in particular Cu. In the thylakoids, PSII has frequently been identified to be the main target. The exact location of its damage, however, strongly depends on the irradiance conditions, as shown originally by Cedeno-Maldonado et al. (1972) and later by Küpper et al. (1996b, 1998, 2002). The latter authors found that in low irradiance including a dark phase, the inhibition of PSII is largely due to the impairment of the correct function of the light-harvesting antenna; this mechanism was termed "shade reaction." It results from the substitution by heavy metals of the Mg^{2+} ion in the chlorophyll (Chl) molecules of the light-harvesting complex II. In high irradiance, direct damage to the PSII reaction center (RC) occurs instead, which most likely involves insertion of Cu^{2+} into the Pheo *a* of the PSII RC. This was

[1] This work was supported by the Stiftung Umwelt und Wohnen and the Fonds der Chemischen Industrie (grant no. 661278 to H.K.), by the European Community "Access to Research Infrastructure Action of the Improving Human Potential Programme" to the EMBL Hamburg Outstation (contract no. HPRI–CT–1999–00017), and by Konstanz University.

* Corresponding author; e-mail hendrik.kuepper@uni-konstanz.de.

The author responsible for distribution of materials integral to the findings presented in this article in accordance with the policy described in the Instructions for Authors (www.plantphysiol.org) is: Hendrik Küpper (hendrik.kuepper@uni-konstanz.de).

[W] The online version of this article contains Web-only data.

[OA] Open Access articles can be viewed online without a subscription.

www.plantphysiol.org/cgi/doi/10.1104/pp.109.139717

named "sun reaction" (Küpper et al., 1996b, 1998, 2002). Also, oxidative stress has often been described as a result of Cu stress; recent data have shown that in photosynthetic organisms, it is mainly a consequence of an inhibition of the photosynthetic light reactions (Rocchetta and Küpper, 2009).

Plants developed a number of strategies to resist the toxicity of heavy metals, as reviewed by Cobbett and Goldsbrough (2002) and Küpper and Kroneck (2005). Such strategies include efflux pumps, sequestration in cells and intracellular compartments where metals do least harm, and binding of heavy metals inside the cells by strong ligands like phytochelatins or free amino acids. A majority of the heavy metal-resistant plants, called "excluders," prevent the accumulation of heavy metals inside their tissues (Baker, 1981). Other resistant plants actively take up heavy metals, translocate them into the shoot, and sequester them to certain parts of the plant, where they are stored in a harmless state. These plants, which accumulate up to several percent of heavy metals in the dry mass of their aboveground parts, are called "hyperaccumulators" (Brooks et al., 1977). In their natural habitats, metal-rich soils in many parts of the world, this type of heavy metal accumulation serves as a defense against pathogens and herbivores (Boyd and Martens, 1994; Martens and Boyd, 1994; Boyd et al., 2002; Hanson et al., 2003; Jhee et al., 2005). They can now be used for the decontamination ("phytoremediation") of anthropogenically heavy metal-contaminated soils and in some cases also for the commercial extraction ("phytomining") of high-value metals (mainly Ni) from metal-rich soils (Baker et al., 1994; McGrath and Zhao, 2003; Chaney et al., 2005).

The mechanisms by which hyperaccumulator plants accumulate the enormous amounts of heavy metals in their shoots and prevent phytotoxicity of these metals have been the subject of many studies. Nevertheless, many of these mechanisms are still under debate (Pollard et al., 2002; Küpper and Kroneck, 2005), and a short overview is given in our companion article (Mijovilovich et al., 2009) on Cu in the Cd/Zn model hyperaccumulator plant *Thlaspi caerulescens*. Studies of arsenic, Cd, Ni, and Zn binding in hyperaccumulators (Krämer et al., 1996; Sagner et al., 1998; Salt et al., 1999, Wang et al., 2002; Küpper et al., 2004) indicated that in such plants most of the metals are coordinated by organic acids, which are commonly found in plant vacuoles. Nonaccumulator plants, in contrast, are well known to bind heavy metals by strong sulfur ligands such as phytochelatins (mainly for Cd) and metallothioneins (mainly for Cu), as reviewed by Cobbett and Goldsbrough (2002).

While hundreds of species have been found to hyperaccumulate Ni and about two dozen to hyperaccumulate Zn, true Cu hyperaccumulation in the sense of reaching thousands of ppm in the shoot dry weight has rarely been confirmed. Most species reported to be Cu hyperaccumulators before were later found to be false positives due to Cu adsorption on the leaf surface, et cetera; actually, none of the species recently revisited had a bioaccumulation factor larger than 1, which is commonly regarded as a necessary prerequisite of true hyperaccumulation (Faucon et al., 2007). But it is important in terms of the general understanding of metal metabolism in plants to identify how plants can cope with Cu toxicity other than excluding it from their metabolism and how far the mechanisms of Cu detoxification and Cu stress differ in Cu-resistant and -accumulating plants from Cu excluders and Cu-sensitive plants. Such questions are important also for breeding better Cd/Zn hyperaccumulators, since such plants (e.g. *T. caerulescens*) turned out to be Cu sensitive, limiting their phytoremediation potential on soils with mixed contamination (Walker and Bernal, 2004). We now analyzed Cu accumulation and Cu stress in a so far not well-characterized species, the amphibious *Crassula helmsii*, an aggressively invasive plant in Europe (Küpper et al., 1996a). We chose this plant because in a previous study it had turned out to be much more Cu resistant than all other investigated species (Küpper et al., 1996b), but more in summer than in winter. Moreover, preliminary experiments indicated that under high temperatures and salinity, *C. helmsii* switches to circadian acid metabolism (CAM), which might cause its elevated Cu resistance in summer due to the enhanced availability of malate as a Cu ligand. CAM metabolism was first reported for *C. helmsii* by Newman and Raven (1995).

In this study, we investigated physiological mechanisms of Cu-induced inhibition of photosynthesis, Crassulacean acid metabolism induction, and Cu accumulation and complexation in *C. helmsii*. The most important method for our investigations of Cu stress was the two-dimensional (imaging) and spectrally resolved microscopic in vivo measurement of the transients of Chl variable fluorescence in the fluorescence kinetic microscope (FKM; Küpper et al., 2000a, 2007a). Cu ligands were investigated via EXAFS (Table I) measurements, which is an element-specific method and therefore particularly suited for analyzing the in vivo ligands by applying it to intact frozen plant tissues. The FKM and EXAFS measurements were supplemented with measurements of Cu accumulation and CAM induction, a detailed analysis of changes in pigment composition, and measurements/observations of growth.

RESULTS

Plant Growth and Metal Uptake; Visible Symptoms of Cu Stress

Plants treated with toxic levels of Cu showed bleaching of leaves, and plants of the emerged cultures additionally wilted (Fig. 1). The latter led to a much stronger decrease of fresh weight in response to Cu stress in emerged compared with submerged plants

Table I. *Explanation of technical terms*

Technical Term	Definition/Explanation
Antenna connectivity	The likelihood of energy transfer between antennae of different photosystems (PSII and/or PSI)
CA	Component analysis. In this study, we use this term for the fitting of EXAFS spectra with a linear combination of the EXAFS spectra of model compounds.
EXAFS	Extended x-ray absorption fine structure
F_0	Minimal fluorescence yield of a dark-adapted sample, fluorescence in nonactinic measuring light
F_m	Maximum fluorescence yield of a dark-adapted sample after supersaturating irradiation pulse
F_m'	Maximum fluorescence yield of a light-adapted sample after supersaturating irradiation pulse
F_v/F_m	$(F_m - F_0)/F_m$ = maximal dark-adapted quantum yield of PSII photochemistry
F_p	Fluorescence yield at the P level of the induction curve after the onset of actinic light exposure
Light saturation	Measured by the increased amplitude of F_p relative to F_m after subtraction of F_0. $(F_p - F_0)/(F_m - F_0)$ is mostly dependent on the ratio of functional antenna molecules to functional RCs and electron transport chains. Under constant actinic irradiance for measuring F_p, a large antenna capturing photons and delivering them to its RC will cause more of the "electron traffic jam" that leads to F_p than a small antenna.
Φ_{PSII}	$\Phi e = (F_m' - F_t')/F_m'$ = the light-acclimated efficiency of PSII (Genty et al., 1989). In this article, the use of this parameter is extended to the relaxation period after the end of actinic light to analyze the return of the system to its dark-acclimated state as measured by F_v/F_m.
NPQ	Nonphotochemical quenching, in this article used as an acronym for the name of this phenomenon. In this article, we measure nonphotochemical quenching as $q_{CN} = (F_m - F_m')/F_m$ = "complete nonphotochemical quenching of Chl fluorescence," i.e. with normalization to F_m.
Pheo	Pheophytin
XAS	X-ray absorption spectroscopy
Z	Atomic number

(Table II). Surprisingly, nevertheless, the Cu content per dry weight was the same for both submerged and emerged Cu-stressed plants, and in both cases it reached more than 9,000 ppm (Table II). In the low-Cu control plants, emerged plants contained about 35% more Cu than submerged plants. Cu concentrations in the plants increased almost proportionally, with only little saturation, in relation to Cu concentrations in the nutrient solution. In the emerged plants, the 100-fold increase of Cu between the controls and the stressed plants yielded a 73-fold increase of Cu in the plant dry weight, while in the submerged plants, it resulted in a 97-fold increase in plant Cu content (Table II).

Pigments

Pigment contents mainly varied between control and Cu-stressed plants, with the latter generally having less of all pigments. Surprisingly, no remarkable Cu-induced changes in the ratio of Chl to carotenoids were found, and the ratio Chl *a*/Chl *b* decreased only slightly (Fig. 2), although Chl *b* is generally known to be more stable toward degradation. Only a somewhat slower degradation of β-carotene-like pigments (β-carotene and zeaxanthin) compared with other carotenoids under Cu stress was found. The substitution of Mg^{2+} in Chl by Cu (i.e. formation of [Cu(II)]-Chl) was barely above the noise limit of this quantification (Fig. 2). Only in samples of plants from the submerged stock cultures was a clear formation of about 2% [Cu(II)]-Chl *a* compared with total Chl *a* found. In the samples from emerged stock culture, the noise of this quantification was too high for unknown reasons (possibly formation of unknown compounds). [Cu(II)]-Chl *b* was never detected. Interestingly, some differences in pigmentation were found when comparing control plants in the submerged versus emerged state, although the submerged plants were only a few centimeters below the water surface, so that light absorption should be minimal. Regardless of preculture conditions, control plants that were grown in the submerged state during the experiment duration had a higher content of Chl *a* and Chl *b* (but no difference in their ratio) and a slightly lower Chl/carotenoid ratio (Fig. 2, bottom panels) compared with plants grown in the emerged state. The lower Chl/carotenoid ratio was due to a much lower content of β-carotene-like pigments in the emerged plants, while levels of all other carotenoids were identical in the emerged versus submerged state (Fig. 2, top panels).

Photosynthesis

pH Measurements of CAM

The results of pH measurements of *C. helmsii* leaves for detecting circadian changes of acid content indicative of CAM are shown in Figure 3.

Both in the plants from submerged and emerged stock culture, the leaves of emerged plants were more acidic in the evening. The difference between the pH in the morning and in the evening, however, was larger in the submerged compared with the emerged plants. All plants from submerged stock cultures had a higher pH in the evening compared with plants from emerged stock culture. Compared with the corre-

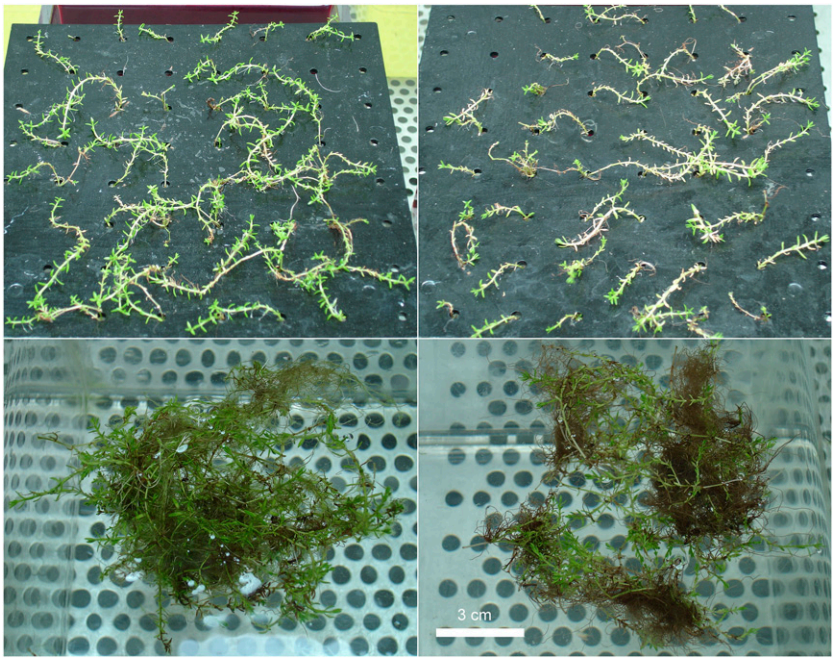

Figure 1. Photographs of plants (emerged stock culture) after 1 week of treatment. Top panels, Emerged treatments; bottom panels, submerged treatments; left panels, control (0.1 μM Cu^{2+}); right panels, stressed with 10 μM Cu^{2+}.

sponding controls, the Cu-stressed plants of the emerged stock cultures had higher pH differences, independent of whether they were emerged or submerged during the experiment. Surprisingly, the opposite was observed for plants from submerged stock culture; in this case, Cu stress diminished the pH difference between morning and evening. In contrast to all other trends, the effects of Cu stress on the pH difference were too small to be statistically significant (ANOVA at $P = 0.05$; $n = 16$ independent treatments).

$\delta^{13}C$ Measurements of CAM

The Cu concentration did not have a significant influence on the carbon isotope pattern of *C. helmsii*. Within a series of incubations (three to four replicates), the ΔPDB value remained within −26 to −27 in both control conditions (0.1 μM Cu^{2+}) and treatment with elevated Cu^{2+} levels (10 μM), irrespective of whether a culture was submerged or emerged (Table II).

Fluorescence Kinetics

Cu-induced changes in Chl fluorescence kinetics are shown in Figure 4, with the kinetics themselves being shown in Figure 4B and the parameter values derived from them shown in Figure 4A. The response of the leaves was rather homogeneous (Supplemental Fig. S2), in contrast to the large cell-to-cell differences in Cd-induced inhibition in the Cd/Zn-hyperaccumulator *T. caerulescens* investigated earlier (Küpper et al., 2007a). This homogeneity of the response now was observed for all fluorescence kinetic parameters.

The maximal fluorescence yield (F_m) was higher in plants from submerged stock culture compared with plants from emerged stock culture. It did not change much further, however, during the 10 d of the experimental conditions irrespective of the growth state (submerged or emerged) during this time. The basic fluorescence yield (F_0), in contrast, decreased during this time if plants from submerged stock culture were grown in the emerged state during the experiment (treatments ECt and ECu in the left column of Fig. 4A). Cu stress never had any significant (*t* test, $P = 0.05$) influence on F_0 or F_m levels.

The maximum quantum yield of charge separation in the PSII RC, as measured by $F_v/F_m = (F_m - F_0)/F_m$, reflected the changes of F_0 and F_m as mentioned above (i.e. it was lower in the submerged compared with the emerged growth state and increased if plants from submerged stock culture were transferred to the emerged conditions). In contrast, F_v/F_m was not sig-

Table II. *Cu concentrations, plant growth, and carbon isotope discrimination in the plant samples*
The values are averages and SE of three to four independent experiments.

Sample	Cu	Shoot Fresh Weight	Average $\delta^{13}C$
	mg/g	*% of control*	
10 μM Cu^{2+}, emerged culture	9,200 ± 1,500	66.8 ± 9.2	−26.65 ± 1.69
10 μM Cu^{2+}, submerged culture	9,100 ± 800	97.7 ± 3.8	−26.33 ± 1.75
0.1 μM Cu^{2+}, emerged culture	127 ± 12	100 per definition	−27.21 ± 1.31
0.1 μM Cu^{2+}, submerged culture	93 ± 3	100 per definition	−26.15 ± 1.45

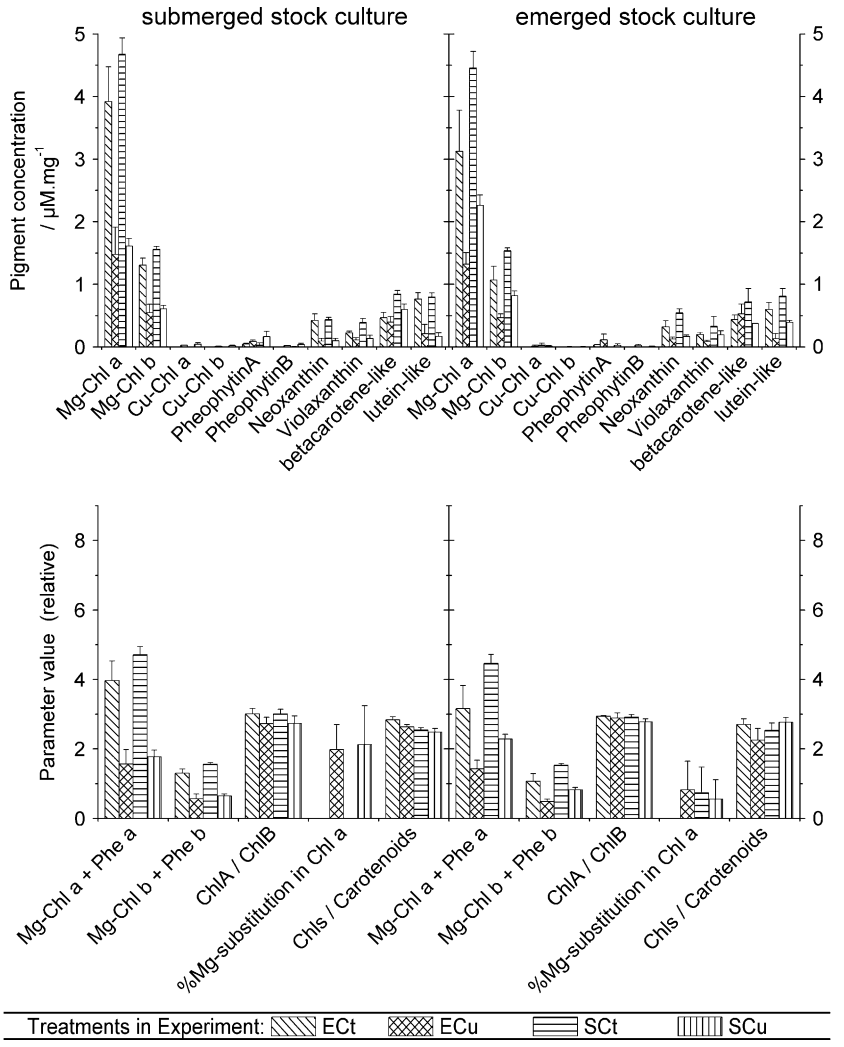

Figure 2. Changes in pigment contents in *C. helmsii* leaves as a result of emerged versus submerged growth and Cu stress. The data are averages and SE of three independent experiments. Treatment labels are as follows: E, experiment (treatment) in emerged state; S, experiment in submerged state; Cu, treated with 10 μM Cu^{2+}; Ct, control (0.1 μM Cu^{2+}).

nificantly (*t* test, $P = 0.05$) affected by the Cu treatment except for the submerged plants from emerged stock culture, where a decrease of F_v/F_m was observed (Fig. 4A, right column).

Photochemical yield of PSII in the light-acclimated state, as measured by $\Phi_{PSII} = (F_m' - F_t')/F_m'$ (Genty et al., 1989), with saturating irradiation pulses (SIPs) i1 to i4 in our protocol (see "Materials and Methods"), generally decreased in response to Cu stress if plants of the stock cultures were grown in the submerged state (Fig. 4A, left panels). In plants from submerged stock culture, this inhibition was much weaker than in plants from emerged stock culture, and the inhibition was only visible at the beginning of the actinic light phase of the measuring protocol (i.e. measurements with SIPs i1 to i3; Fig. 4). In contrast, in the plants from emerged stock culture, the inhibition of Φ_{PSII} remained visible throughout the measurement (Fig. 4). No effect of Cu on Φ_{PSII} was found in plants that were stressed with Cu in the emerged state regardless of the preculture conditions.

Nonphotochemical quenching of Chl fluorescence, measured as NPQ = $(F_m - F_m')/F_m$, increased in response to Cu stress under most conditions analyzed (Fig. 4A). This was more pronounced in plants from emerged stock culture (Fig. 4A, right column) compared with plants from submerged stock culture (Fig. 4A, left column). In the latter, no Cu-induced increase in NPQ was found in the completely light-acclimated state (SIP i4), and after the end of the actinic light period of the measurement even a decrease of NPQ in response to Cu stress was found (SIPs r1 and r2 in Fig. 4).

The most consistent results were obtained for the light saturation parameter $(F_m - F_0)/(F_p - F_0)$, which is a measure of the ratio between functional antenna complexes to functional PSII RCs (Küpper et al., 2007a). In all plants from both stock cultures, this parameter always increased in response to Cu toxicity stress. The extent of this increase, however, strongly varied dependent on the precultivation of the stock culture; it was much stronger in plants from submerged stock culture compared with emerged stock culture (Fig. 4A). Among the plants of the submerged stock culture, the Cu-induced increase in light saturation was stronger when they were treated with Cu in

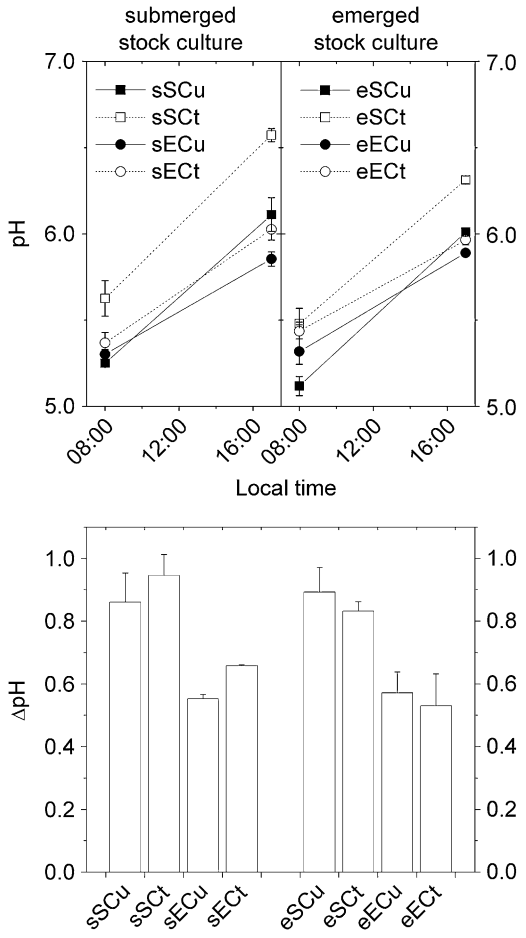

Figure 3. Results of pH measurements of *C. helmsii* leaves for detecting circadian changes of acid content indicative of CAM. The lines between the morning and evening measuring points are only a visual aid for making it easier to see which pairs of points belong together; they do not imply that there would be a linear decrease of pH over the day. The data are averages of two independent experiments. Treatment labels are as follows: e, emerged stock culture; s, submerged stock culture; E, experiment (treatment) in emerged state; S, experiment in submerged state; Cu, treated with 10 μM Cu^{2+}; Ct, control (0.1 μM Cu^{2+}).

the submerged state than when they were treated with Cu in the emerged state. This, however, was not caused by a higher degree of light saturation in these Cu-treated plants but by a lower light saturation of the controls of the submerged compared with the emerged treatment of plants from submerged stock culture.

EXAFS Measurements

Model Compounds

For aqueous Cu^{2+} (prepared by dissolving $CuSO_4$) as well as for Cu(II)-malate and Cu(II)-citrate, the best fit was for four low-Z ligands (oxygens were tried) bound to Cu at a regular distance, plus possibly one or two long-distance low-Z ligands (Supplemental Fig. S1; Supplemental Tables S1 and S2). For aqueous Cu^{2+}, these ligands would be the oxygen atoms from water molecules, while for the organic acid complexes, they would be carboxyl oxygens.

Plant Samples

The main feature was the almost complete lack of sulfur ligands and Cu-Cu interactions. In all *C. helmsii* samples, Cu was only coordinated to low-Z ligands. This was revealed by both the EXAFS refinements (Table III; Fig. 5) and the component analysis (data not shown). In the spectra, there was a small contribution from higher shells. Attempts to fit a nicotianamine contribution in the refinements showed on average half a nicotianamine per Cu ion, and the SE values indicated that this was not above the noise level. Similarly, the component analysis did not reveal any nicotianamine contribution above the noise level (<4%), and the contribution of His was not significant (not detectable in emerged plants, 4.9% ± 4.9% in submerged plants).

DISCUSSION

The analyses of total metal content in the plant samples clearly showed that *C. helmsii* is a Cu hyperaccumulator, with Cu contents far higher than in previously reported Cu hyperaccumulators. This makes *C. helmsii* an attractive plant for studying Cu metabolism in plants, in particular in comparison with plants with different Cu sensitivity and accumulation, which is the main reason for linking this article with the one on Cu metabolism in the Cu-sensitive Cd/Zn hyperaccumulator *T. caerulescens*. In contrast to other hyperaccumulators, where higher (than in related nonaccumulator plants) requirements for the hyperaccumulated metals were found (Shen et al., 1997, for Zn in *T. caerulescens* and Küpper et al., 2001, for Ni in three hyperaccumulator species), there seems to be no higher Cu requirement in *C. helmsii*. The 0.1 μM was sufficient both for *C. helmsii* as a Cu accumulator and for *T. caerulescens* as a nonaccumulator for Cu. Studying Cu accumulation, binding, and toxicity in *C. helmsii* has revealed features that distinguish it from plants with different responses to Cu (e.g. *T. caerulescens*) but also revealed some similarities.

Cu-Induced Inhibition and Submerged/Emerged Adaptation of Metabolism

Pigment Changes

Surprisingly, no Cu-induced changes in the ratio of Chl to carotenoids, and only a small decrease of the Chl *a*/Chl *b* ratio, were found in response to Cu stress, although these pigments usually have a different lifetime during decay, leading to autumnal coloring of leaves (Wolf, 1956; Sanger, 1971). This is in line with the observation that *C. helmsii* leaves dying from Cu

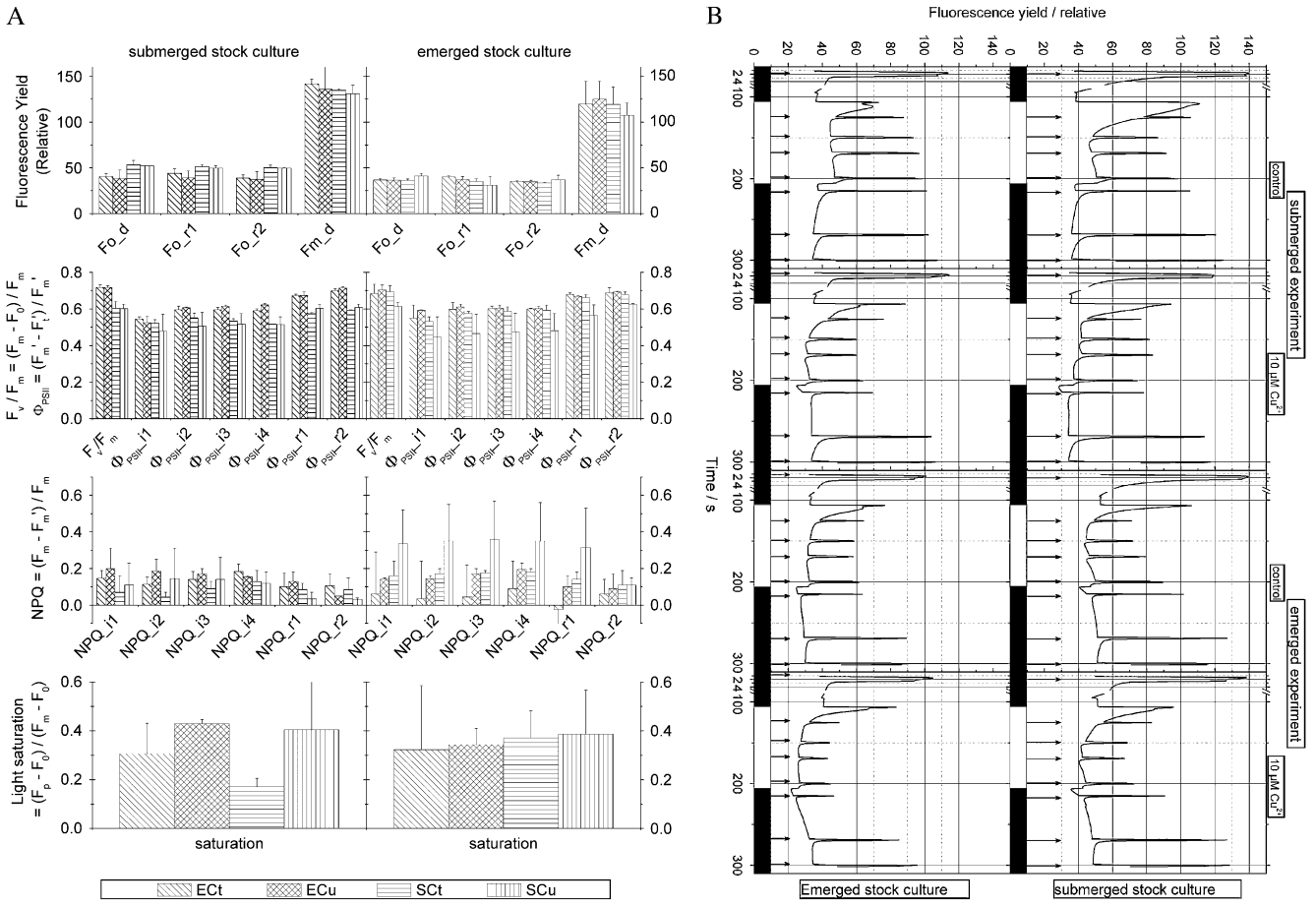

Figure 4. Changes in the biophysics of photosynthesis as a result of emerged versus submerged growth and Cu stress, revealed by Chl fluorescence parameters. All samples were measured in the FKM at an actinic irradiance of 120 μmol m^{-2} s^{-1}. See "Materials and Methods" for details of the measuring protocol, including timing of events. The data are averages of two independent experiments. Treatment labels are as follows: E, experiment (treatment) in emerged state; S, experiment in submerged state; Cu, treated with 10 μM Cu^{2+}; Ct, control (0.1 μM Cu^{2+}). A, Selected parameters. Indices of sections of the measuring protocol are as follows: "_d" stands for "dark adapted," "_i" stands for "irradiated with actinic light," and "_r" stands for "relaxation period after actinic irradiance." The numbers in the index sequentially number the SIPs in the respective protocol section. A short explanation of individual fluorescence kinetic parameters is provided in Table I; for details, see reviews on Chl fluorescence kinetics or Küpper et al. (2007a). Top row, Basic parameters of fluorescence yield in nonactinic (F_0) and supersaturating (F_m) light; second row, parameters measuring photochemical activity (F_v/F_m and Φ_{PSII}); third row, parameters measuring NPQ; bottom row, light saturation as measured by F_p in relation to F_m with correction of F_0 effects. B, Typical examples of complete fluorescence kinetic measurements. See "Materials and Methods" for details of the measuring protocol, including timing of events. The black bars at the bottom of the panels indicate periods of the measurement when actinic light is switched off, and the white bars symbolize the time period of actinic irradiance. The arrows indicate the positions of the SIPs.

stress bleached very quickly and showed an unusually rapid, and therefore most likely active, degradation of all pigments once a cell has died from Cu stress. This could be an emergency defense mechanism against Cu stress in *C. helmsii*, since sacrificing some leaves as Cu dumps with recovery of nutrients from them could decrease Cu stress in the remaining tissues.

The decrease of Chl content in emerged compared with submerged plants indicates that in the emerged state, *C. helmsii* "anticipates," via a regulatory mechanism, high-light stress in the emerged state and light limitation in the submerged state, even if in the experimental conditions the plants were only a few centimeters below the water surface so that light absorption by water should be minimal. This correlates with changes in photosynthesis, as discussed below. It remains unclear, however, why the content of light-protective β-carotene-like carotenoids decreased in the emerged state.

Biophysics of Photosynthesis and CAM

The most noticeable Cu-induced change in photosynthetic parameters was the increase of the degree of light saturation, which was found in all analyzed treatments (although with different amplitudes). This

Table III. *Results of the refinement of the EXAFS spectra using the DL-Excurve program*

Nitrogen and oxygen are used indistinctively, since their scattering phases are similar. The graphs of the fits for the model compounds are shown in Supplemental Figure S1, and those of the plant samples are shown in Figure 5. The refinement parameters of the model compounds are shown in Supplemental Table S1. The refinements of model compounds that were more relevant for *T. caerulescens* [Cu (I/II)-glutathione, Cu(II)-His, Cu(II)-nicotianamine, and Cu(II)-Pro] are shown in the companion article (Mijovilovich et al., 2009) about Cu metabolism in that species. eSCu, *C. helmsii* from emerged stock culture treated with Cu in the submerged state; sSCu, *C. helmsii* from submerged stock culture treated with Cu in the submerged state; eECu, *C. helmsii* from emerged stock culture treated with Cu in the emerged state; sECu, *C. helmsii* from submerged stock culture treated with Cu in the emerged state; EF, Fermi energy shift with respect to E0 = 8,979 eV used in the background subtraction, which defines the threshold for the EXAFS spectra (Rehr and Albers, 1990; this value was refined for every sample); FI, fit index; SE, mathematical SE values of the refinement (2σ level). The error of the EXAFS approach as such is higher; this is revealed by the differences between samples of the same type. Asterisks indicate values that were constrained to be identical for these contributions. Deviations from this simplification do not improve the model significantly. NA, Nicotianamine.

Sample	No., Type of Ligands ±SE	Distance ± SE	$2\sigma_i^2$ ± SE	EF ± SE	FI
		Å	Å^2		
eSCu	5.2 ± 0.4, O	1.948 ± 0.002*	0.008 ± 0.001*	−12.8 ± 0.5	0.180
	0.4 ± 0.5, NA	1.948 ± 0.002*	0.008 ± 0.001*		
	0.1 ± 0.3, S	2.477 ± 0.221	0.008 ± 0.001*		
sSCu	4.9 ± 0.5, O	1.941 ± 0.008*	0.009 ± 0.002*	−11.3 ± 0.4	0.138
	0.6 ± 0.6, NA	1.941 ± 0.008*	0.009 ± 0.002*		
	0.3 ± 0.1, S	2.467 ± 0.027	0.009 ± 0.002*		
eECu	3.3 ± 0.8, O	1.919 ± 0.008*	0.004 ± 0.002*	−9.1 ± 1.1	1.077
	0.6 ± 0.6, NA	1.919 ± 0.008*	0.004 ± 0.002*		
	0.4 ± 0.2, S	2.344 ± 0.037	0.004 ± 0.002*		
sECu	5.1 ± 0.5, O	1.940 ± 0.008*	0.009 ± 0.001*	−11.2 ± 0.4	0.140
	0.5 ± 0.6, NA	1.940 ± 0.008*	0.009 ± 0.001*		
	0.4 ± 0.2, S	2.473 ± 0.029	0.009 ± 0.001*		

shows a decreasing number of functional RCs or PSII → PSI electron transport chains relative to the antenna, if the photosynthetic system has a high antenna connectivity, so that each antenna molecule may deliver its excitons to different RCs. Interestingly, this Cu-induced increase in light saturation was much stronger in plants from submerged compared with emerged stock culture and stronger if Cu stress was applied in the submerged than in the emerged state.

The Φ_{PSII} decreased in response to Cu, particularly at the beginning of actinic irradiance, indicating that later on a rearrangement of the photosynthetic system could alleviate some of the defects caused by Cu toxicity. This did not apply, however, to those mechanisms that led to an increased nonphotochemical fluorescence quenching during Cu stress, as that increase remained constant throughout the actinic light period. This different behavior of changes in photochemistry and nonphotochemical quenching shows again, as in our previous study on Cd stress in *T. caerulescens* (Küpper et al., 2007a), that these two parts of photosynthesis biophysics represent different targets (proteins) affected by heavy metal (Cd and Cu) toxicity.

A common observation in many earlier studies of Cu stress with ecologically plausible concentrations of Cu^{2+} (Lanaras et al., 1993; Lidon et al., 1993; Ouzounidou et al., 1995, 1997; Ouzounidou, 1996) was that Cu^{2+} usually does not affect the maximum dark-adapted quantum yield of PSII, measured as F_v/F_m. If Cu stress is investigated under high-irradiance conditions or with long light phases, however, the situation is often different. This was first found by Lanaras et al. (1993) in leaves of *Triticum aestivum*, where Cu toxicity caused a considerable decline of F_v/F_m, resulting from both an increase of F_0 and a decrease of F_v. Similar effects were found by Küpper et al. (1998, 2002, 2003) in green and red algae under Cu stress, where they could be linked to inhibition of the PSII RC likely by insertion of Cu^{2+} into the Phe *a* in the sun-reaction type of damage (Küpper et al., 2002). In this study, F_v/F_m did not decrease, although the changes in light saturation, the visual damage symptoms, and pigment changes now resembled the sun reaction. In previous studies, it was often concluded from such nondecreasing F_v/F_m that Cu^{2+} would not affect the efficiency of the primary photochemistry in PSII of the dark-adapted leaf cells. This conclusion, however, is not reliable. [Cu(II)]-Chl is both nonfluorescent and a very strong quencher of excitons transferred to it from magnesium (Mg)-Chl in the same photosystem, as discussed in detail by Küpper et al. (2002). Therefore, insertion of Cu^{2+} in the Phe *a* of the PSII RC during sun reaction makes the affected PSII RCs nonfluorescent (i.e. the Cu-inhibited photosystems do not contribute to the measurable Chl *a* fluorescence and thus F_v/F_m). But in a system with high antenna connectivity, as seems to be the case here, they lead to the observed

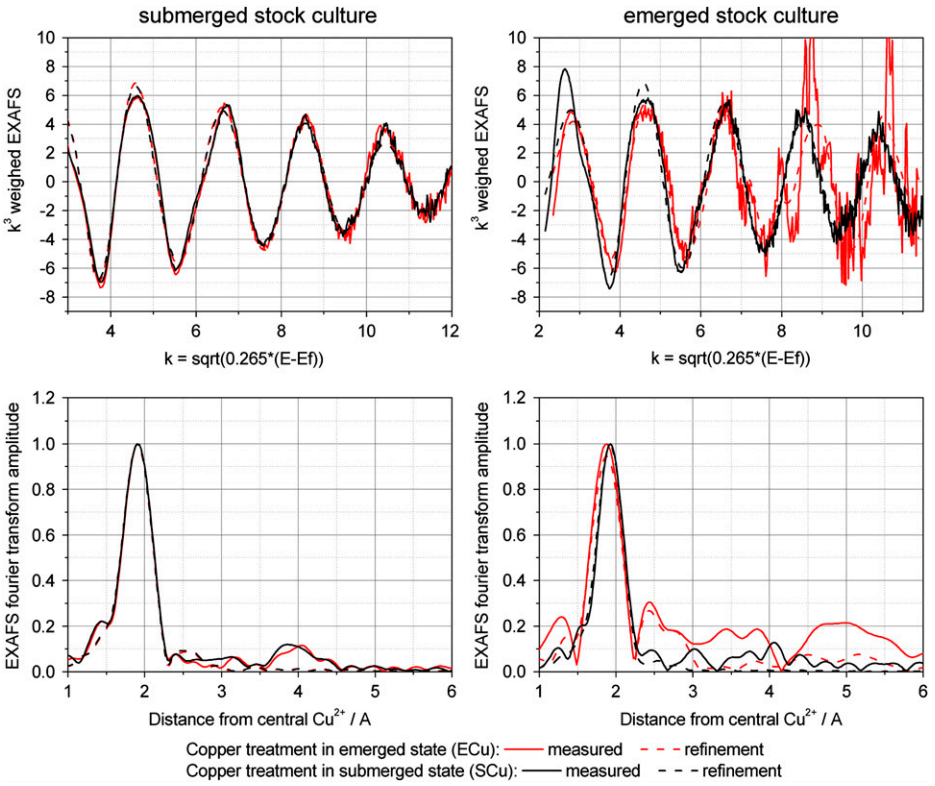

Figure 5. Spectra of in situ x-ray absorbance measurements (Cu-K edge) of frozen-hydrated *C. helmsii* tissues. Treatment labels are as follows: Ef, Fermi energy (Rehr and Albers, 1990); E, experiment (treatment) in emerged state; S, experiment in submerged state; Cu, treated with 10 μM Cu^{2+}; Ct, control (0.1 μM Cu^{2+}). Top, Normalized EXAFS and fit with theoretical model. Bottom, Fourier transform of the EXAFS and fits with theoretical model (done on normalized EXAFS).

higher degree of light saturation (see above), since the unchanged antenna now delivers its excitons to a lower number of functional RCs.

The aforementioned effects of Cu on light saturation and Φ_{PSII} clearly showed that in submerged conditions, *C. helmsii* changes its metabolism in a way that makes it more susceptible to Cu stress. This is in line with our earlier observations (H. Küpper and F.C. Küpper, unpublished data) that *C. helmsii* is more Cu resistant in summer, when most of the population is above the water level of the drying-out ponds, than in winter, when most of the population is submerged. This difference in Cu sensitivity cannot be due to stronger Cu uptake in submerged conditions, as the Cu content of the Cu-stressed plants was identical in the submerged and emerged states. Rather, it must be a change in metabolism. We previously suspected that this change in resistance could be due to the (stronger) induction of CAM in response to temperature and salinity in summer; therefore, we analyzed CAM now via pH measurements of acid consumption during the day and via carbon isotope discrimination ($\Delta^{13}C$) measurements. While the pH measurements now clearly indicated that *C. helmsii* performed CAM, the $\Delta^{13}C$ values were always in the range of regular C3 photosynthesis. The reason for this discrepancy remains unclear. The pH difference of the control plants was much stronger in the submerged compared with the emerged state, indicating stronger CAM in the former. These results clearly show that CAM does not protect against Cu toxicity but rather makes the plants more susceptible to it. The mechanism of the latter remains to be solved in the future. The extent of diurnal pH change indicative of CAM was most influenced by the conditions during the experiment, but the preculture conditions still influenced this, in two ways. First, as expected, control plants grown in the experiment in the submerged or emerged state displayed a larger pH difference if they were pregrown in the submerged state. Second, surprisingly, the preculture condition inverted the effect of Cu stress on the pH difference. In both emerged and submerged plants from submerged preculture, Cu stress decreased the pH difference, while in plants from emerged preculture, Cu increased the pH difference (i.e. CAM). This indicated that Cu influences the intricate regulation of CAM versus C3 photosynthesis on *C. helmsii*, which is, to our knowledge, a previously unknown effect of Cu toxicity.

Metal Speciation and Detoxification in Hyperaccumulators

In *C. helmsii*, in contrast to *T. caerulescens* (see Mijovilovich et al., 2009), Cu was bound almost exclusively by oxygen ligands, without any measurable contribution of sulfur ligands or Cu-Cu interactions. This resembles the situation in all hyperaccumulators for other metals studied so far, such as Cd and Zn in *T. caerulescens* (Salt et al., 1999; Küpper et al., 2004) and *Arabidopsis halleri* (Sarret et al., 2002), Ni in various species (Krämer et al., 1996; Sagner et al., 1998), and the metalloid arsenic in *Pteris vittata* (Webb et al., 2003; Zhao et al., 2003). These oxygen ligands of Cu in *C.*

helmsii may be organic acid anions like malate or citrate, but unlike in *T. caerulescens*, no major proportion of Cu was bound by nicotianamine. Altogether, *C. helmsii* seems to treat Cu in the same way as hyperaccumulators of other metals do for the metals they accumulate: keep the hyperaccumulated metal out of the cytoplasm and sequester it into the vacuole (most metals, including Cd, Ni, and Zn) or cell wall (shown mainly for aluminum; Carr et al., 2003), as described in the introduction. In the vacuole and cell walls, usually no really strong ligands (e.g. phytochelatins, metallothioneins, nicotianamine, and His) are present, so the metals are only associated with the weak oxygen ligands that are abundant in these compartments (i.e. mainly organic acids like malate and citrate in the vacuole or cellulose in the cell wall). In nonaccumulators, in contrast, metals seem to be mainly detoxified by binding to the strong ligands just mentioned, which seems also to apply to Cu in *T. caerulescens* as a nonaccumulator for this metal (see Mijovilovich et al., 2009). This article and the companion article (Mijovilovich et al., 2009) yielded strong new evidence that these are general principles, as we could show that (1) the same metal, Cu, is bound by weak ligands when looking at a Cu hyperaccumulator (*C. helmsii*) but bound by strong ligands in a Cu nonaccumulator (*T. caerulescens*); and (2) in the same plant (*T. caerulescens*), the hyperaccumulated Cd is bound by weak ligands (Küpper et al., 2004), while the nonaccumulated Cu is bound by strong ligands (see Mijovilovich et al., 2009). In contrast to what could be expected in view of the metabolism of *C. helmsii*, which carries out more CAM photosynthesis in the submerged than in the emerged state, no differences in Cu ligands were found between these two physiological states. This could be because the concentration of organic acids in these plants is always so high that it is not limiting for Cu complexation. Combined with the CAM data mentioned above, it could be that CAM induction does not lead to an overall increase of organic acid content in *C. helmsii* but to a change in acid composition (e.g. a shift from citrate to malate). Such a change would not be detectable by EXAFS, as both Cu complexes have almost the same spectra, but could explain the lower Cu resistance of CAM-performing *C. helmsii*, as malate (two carboxyl groups) binds Cu less strongly than citrate (three carboxyl groups).

In summary, *C. helmsii* turned out to be a very interesting case for studying Cu accumulation, binding, and toxicity in a plant that is both Cu tolerant and Cu accumulating. The latter feature, however, should not be used for phytoremediation attempts, not only because of the small size of this plant but mainly because this species is a very aggressively invasive neophyte, which has already caused severe problems in Europe. The question whether the invasiveness of *C. helmsii* and the decline of the related European species *C. aquatica* are related to different heavy metal resistance is an interesting topic for future investigations. The mechanism of its Cu uptake is an interesting subject for future investigations; one important question to be solved is in how far it involves active transport or passive accumulation via the transpiration stream (emerged state) and binding in the shoot cell walls (submerged and emerged state). Passive Cu accumulation may be much more important than in all terrestrial hyperaccumulators of other metals investigated so far, because in the submerged state the shoot cell walls are in direct contact with the Cu-containing environment, and even in the emerged state the cell walls of this swamp plant may be much more water conductive than in fully terrestrial plants. However, it seems very unlikely that this passive contribution could yield the extremely high accumulation (about 9,000 ppm Cu in the plant dry weight compared with 0.6 ppm in the nutrient solution) that we found in our experiments. Therefore, it seems most likely that the accumulation is by active transport, as was found for all investigated hyperaccumulators of other metals.

MATERIALS AND METHODS

Plant Material, Culture Media, and Culture Conditions

Crassula helmsii was collected from a revegetated dump site for coal mining spoil, General Blumenthal/Schacht 8, in Oer-Erkenschwick, Germany (for details, see Küpper et al., 1996a). For at least 3 months before the experiments, it was grown in the nutrient solution described by Gaudet (1963) with the following modifications: (1) $(NH_4)2Fe(SO_4)2{\cdot}6H_2O$ instead of Fe-EDTA to facilitate heavy metal uptake by the plants; (2) 0.1% of its natural pond water was added; and (3) Cu was omitted from the nutrient solution, since it turned out that the traces of Cu present in other chemicals (about 0.1 μM in the final nutrient solution) were sufficient for healthy growth of *C. helmsii*. During the experiments, the addition of natural pond water was stopped to have more defined conditions, and 10 μM Cu (as $CuSO_4$) was supplied to the plants to be stressed. The nutrient solution was aerated continuously. This Cu concentration was chosen because in preliminary tests it had proven to be sublethally toxic for both organisms that we wanted to compare in this study: *C. helmsii* (this article) and *Thlaspi caerulescens* (Mijovilovich et al., 2009). Using greater Cu concentrations was impossible for practical reasons like availability of pumps and vessels for cultivation (since already eight treatments altogether had to be conducted; Figs. 2–5), measuring time at the FKM, and beamtime at the synchrotron (almost 1 month already, which is longer than most other studies are allowed to take).

We used 7-L vessels, in which the solution was exchanged every 3 to 4 d. For emerged cultivation, 64 plants were placed in holes of a black plastic plate so that the roots were hanging into the nutrient solution. For submerged culture, the plants were allowed to float freely in the nutrient solution. Six separate replicate experiments were performed within 2 years, three of them with emerged and three with submerged stock culture. In each experiment, half of the plants were kept in the condition of the stock culture (emerged or submerged) and the other half were transferred to the other growth condition to simulate the frequent submerged/emerged changes in the natural habitat of this species. Two to 3 weeks after transferring the plants into the pots, 10 μM Cu sulfate was added to the nutrient solution of half of the pots. All plants were grown with 14-h daylength. A 22°C/18°C day/night temperature was applied, and a quasisinusoidal three-step light cycle with about 40 μE in the morning and 120 μE at noon was achieved by full-spectrum discharge lamps. Samples for the various types of analysis (FKM, pigments, EXAFS, atomic absorption spectrometry, $\Delta^{13}C$, tissue pH) were taken 8 $\pm$ 2 d after start of the Cu treatment.

Chl Fluorescence Kinetic Measurements

Here, we performed spatially resolved (two-dimensional, imaging) measurements of Chl fluorescence kinetics via the pulse amplitude modulation principle in the FKM as developed and described by Küpper et al. (2000a,

2007a). For measurements, a leaf was cut off and pressed by its upper side toward the glass window of the measuring chamber (for descriptions, see Küpper et al., 2000a, 2007a) with a wet nylon grid or wet cellophane. The chamber was kept at room temperature (about 20°C) and was ventilated by a stream of air (2 L min^{-1}) saturated with water vapor at the same temperature. Measuring light was less than 1 μE. Blue (410–500 nm) excitation was used, provided by a white light-emitting diode with the excitation filter 2P-HQ 460/80 (AHF; www.ahf.de) and dichroic mirror 505DCXR (AHF). Chl fluorescence was detected from 665 to 705 nm with the emitter D680/30 (AHF).

Measurements lasted 300 s, in the third second of which a short (600-ms) flash of saturating light was given for measurement of F_m (maximum fluorescence yield of a dark-adapted sample), followed by 100 s with neither actinic nor saturating light for measurement of F_0 (the minimal fluorescence yield of a dark-adapted sample; i.e. the fluorescence in nonactinic measuring light). Then, 100 s of actinic light was applied to analyze the Kautsky induction and the degree of light saturation at the beginning of this induction [saturation = $(F_p - F_0)/(F_m - F_0)$] as a measure of functional RCs relative to the size of the connected functional antenna (Küpper et al., 2007a). Finally, again 100 s was measured with no actinic light for measurement of dark relaxation, including F_0' (the minimal fluorescence yield of a light-adapted sample). During the actinic light exposure and in the relaxation period afterward, further 600-ms flashes of saturating light (SIPs) were given in order to measure the photochemistry via Φ_{PSII} [$=(F_m' - F_t')/F_m'$] and NPQ [$=(F_m - F_m')/F_m$]. The flashes during the dark relaxation period were used also to calculate relaxation of Φ_{PSII}. The position of a parameter in the protocol is described by an index behind the main parameter name. Denominators of sections of the measuring protocol are as follows: "_d" stands for "dark adapted," "_i" stands for "irradiated with actinic light," and "_r" stands for "relaxation period after actinic irradiance." The numbers in the index sequentially number the SIPs in the respective protocol section.

The original data (i.e. two-dimensional records of Chl fluorescence kinetics) were analyzed using the FluorCam software from Photon Systems Instruments as described earlier (Küpper et al., 2000a; Ferimazova et al., 2002). The cells used for the statistical analysis were selected to be a representative subset of all cells in the field of view.

Quantification of Chl in Plant Extracts

Shoots were frozen in liquid nitrogen, then lyophilized, and subsequently extracted in 100% acetone. Spectra of pigment extracts were measured with the UV/visible spectrophotometer Lambda 16 (Perkin-Elmer) at a spectral bandwidth of 1 nm with 0.2-nm sampling interval from 350 to 750 nm. Chls were quantified according to the "Gauss-peak-spectra" (GPS) method developed by Küpper et al. (2000b, 2007b). Normalized spectra (350–750 nm) of pigment standards were mathematically described by a series of Gaussian peaks. These GPS were combined to simulate the contributions of possible constituents in the plant extracts, such as Mg-Chl *a*, Mg-Chl *b*, Pheo *a*, Pheo *b*, β-carotene and zeaxanthin (the latter two are subsequently called "β-carotene-like," as their spectra are identical), antheraxanthin and lutein (called antheraxanthin-like in the following, as their spectra are identical), neoxanthin, and violaxanthin. Zeaxanthin and β-carotene, as well as antheraxanthin and lutein, have exactly the same chromophore (π-electron system and functional groups interacting with it), so that their excited states and therefore their absorption and fluorescence spectra are identical. Therefore, also their properties in quenching or harvesting excitation energy (i.e. their relevance in photosynthesis and protection against excess energy) are most likely identical. And for the same reason, it is impossible to distinguish between them by UV/visible spectroscopy. The combinations of GPS were then fitted to the sample spectrum to obtain the parameters representing the concentrations of the individual components. Additionally, baseline drift and wavelength inaccuracies of the spectrophotometer as well as temperature differences, residual water content, and turbidity of the samples were automatically corrected (Küpper et al., 2007b).

Preparation of Plant Samples for EXAFS Measurements

To eliminate problems of element redistribution during sample preparation, the collected tissues were shock frozen in melting nitrogen slush. This slush was generated by pulling a strong vacuum on a container of well-insulated liquid nitrogen (this forces the nitrogen into solid + gaseous state) and then releasing the vacuum, causing the nitrogen "snow" to melt. Afterward, the samples were immediately stored at –80°C. To obtain representative data sets within the limited synchrotron beamtime, aliquots of samples from all plants of the same metal treatment (see above) were mixed, so that each EXAFS sample represented the average of four to eight plants. For the EXAFS measurements, the frozen-hydrated samples were ground to powder in a mortar and filled into EXAFS cuvettes; all this was done at –80°C (dry ice cooling). Afterward, the cuvettes were sealed with Kapton tape and stored in liquid nitrogen.

Preparation of Model Complexes for EXAFS Measurements

A 5 mM solution of $CuSO_4$ was used as reference for the aquo complex. His, citrate, and glutathione complexes with Cu(II) were prepared by adding 50 mM ligand to a 5 mM $CuSO_4$ solution. Our model complexes were acidic, adjusted to pH 4, resembling the situation in plant vacuoles, which are the compartments where plants store organic acids and which are the main sinks for heavy metals in hyperaccumulators (Küpper et al., 1999, 2001). All solutions of the model complexes contained 30% (v/v) glycerol to minimize the formation of ice crystals during freezing. The samples were transferred into EXAFS cuvettes and frozen in liquid nitrogen.

EXAFS Measurements and Data Analysis

Measurements were performed at the EMBL bending magnet beamline D2 (DESY) using a Si(111) double crystal monochromator, a focusing mirror, and a 13-element germanium solid-state fluorescence detector. All samples were mounted in a top-loading closed-cycle cryostat (modified from Oxford Instruments) and kept at about 30 K. The transmitted beam was used for energy calibration by means of the Bragg reflections of a static Si(220) crystal (Pettifer and Hermes, 1985). At least 500,000 counts above the Cu-K absorption edge were accumulated for each measurement. Data reduction and averaging were done using the EXPROG (Korbas et al., 2006) and KEMP (Korbas et al., 2006) packages of programs. Data analysis was performed using DL_Excurv (Tomic et al., 2005), which is a freeware version of Excurve (Binstead et al., 1992) under the flagship of CCP3 (www.ccp3.ac.uk/).

The k-range was chosen according to the statistical quality of the data at the end of the k-range, from 3 $Å^{-1}$ to a higher end at 8.5 to 13 $Å^{-1}$. Since nitrogen and oxygen are indistinguishable by EXAFS due to their similar scattering phases, both elements are used indistinctively when modeling individual ligand shells. But multiple scattering contributions (e.g. of the imidazole ring of His) may allow unambiguous assignment of oxygen versus nitrogen and of ligand molecules (e.g. His, nicotianamine). As His (as free amino acid or in proteins) is the only potential nitrogen ligand that is abundant enough and has a high enough Cu affinity to contribute to Cu binding in plants, His was included in our refinements. His was modeled using the coordinates provided by the DL-Excurve release, and the nicotianamine coordinates were taken from NICOAM01.cif (Miwa et al., 1999). Further details of the nicotianamine refinement are described in our companion article (Mijovilovich et al., 2009) on *T. caerulescens*.

In addition to the refinement described above, the measured EXAFS data of all plant samples were fitted with a linear combination of the measured curves of all model complexes. This fit, subsequently called "component analysis," was done in order to have a second method to estimate the proportions of the different types of ligands around the metals. The fitting of measured XAS sample data by a linear combination of measured model data has also successfully been used by Salt et al. (1999) for Zn in samples of *T. caerulescens* and by Küpper et al. (2004) for Cd and Zn in the same species. In this work, the approach of Salt et al. (1999) was modified as described by Küpper et al. (2004).

Determination of Metals in Whole Plant Tissues

Frozen-hydrated plant samples (see above) were lyophilized, ground, and subsequently digested with a mixture of HNO_3 and $HClO_4$ (Zhao et al., 1994). Concentrations of Cu in the digests were determined using atomic absorption spectrometry in a GBC 932 AA spectrometer (GBC Scientific Equipment).

Measurements of Carbon Isotope Discrimination

Carbon isotope discrimination measurements were carried out as previously described by Flynn and Davidson (1993). In brief, samples were analyzed using a 20-20 stable isotope mass spectrometer (PDZ Europa) with

an ANCA-NT prep system. Freeze-dried and ground plant samples (of around 1 mg target weight) were weighed and enclosed in tin capsules, which were inserted into the instrument for combustion/reduction via an autosampler prior to mass spectrometry. $\delta^{13}C$ values are relative to PDB standards. Instrument calibration was conducted using Ile (Sigma; isotope composition determined by Europa Scientific). $\delta^{13}C$ values are given by $[((^{13}C/^{12}C \text{ sample})/(^{13}C/^{12}C \text{ standard})) - 1] \times 1{,}000$.

Supplemental Data

The following materials are available in the online version of this article.

Supplemental Figure S1. Comparison of Cu XAS of different model compounds.

Supplemental Figure S2. Typical examples of maps of the light saturation parameter $(F_p - F_0)/(F_m - F_0)$ of the fluorescence kinetic measurements after 8 d of treatment (submerged stock culture), showing that the response of the leaves was rather homogeneous, in contrast to the distribution of Cd-induced inhibition in the Cd/Zn-hyperaccumulator plant *T. caerulescens* investigated earlier (Küpper et al., 2007a).

Supplemental Table S1. Table of Cu-EXAFS refinement parameters of the model compounds shown in Supplemental Figure S1.

Supplemental Table S2. Alternative refinements of the plant samples for testing the presence of biomineralization (Cu phosphates, oxalate, and oxides) that was found in the *T. caerulescens* samples in our companion article (Mijovilovich et al., 2009).

ACKNOWLEDGMENTS

We thank Sharon McNeill and Keith Davidson (Scottish Association for Marine Science) for their support with $\delta^{13}C$ measurements. We gratefully acknowledge a generous donation of laboratory equipment from the Degussa-Hüls AG (Infracor GmbH) to H.K.

Received April 9, 2009; accepted July 20, 2009; published July 29, 2009.

LITERATURE CITED

Baker AJM (1981) Accumulators and excluders: strategies in the response of plants to heavy metals. J Plant Nutr **3:** 643–654

Baker AJM, McGrath SP, Sidoli CMD, Reeves RD (1994) The possibility of in situ heavy metal decontamination of polluted soils using crops of metal-accumulating plants. Resour Conserv Recycling **11:** 41–49

Binstead N, Strange RW, Hasnain SS (1992) Constrained and restrained refinement in EXAFS data analysis with curved wave theory. Biochemistry **31:** 12117–12125

Boyd RS, Davis MA, Wall MA, Balkwill K (2002) Nickel defends the South African hyperaccumulator *Senecio coronatus* (Asteraceae) against *Helix aspersa* (Mollusca: Pulmonidae). Chemoecology **12:** 91–97

Boyd RS, Martens SN (1994) Nickel hyperaccumulated by *Thlaspi montanum* var. *montanum* is acutely toxic to an insect herbivore. Oikos **70:** 21–25

Brooks RR, Lee J, Reeves RD, Jaffre T (1977) Detection of nickeliferous rocks by analysis of herbarium species of indicator plants. J Geochem Explor **7:** 49–57

Carr HP, Lombi E, Küpper H, McGrath SP, Wong MH (2003) Accumulation and distribution of aluminium and other elements in tea (Camellia sinensis) leaves. Agronomie **23:** 705–710

Cedeno-Maldonado A, Swader JA, Heath RL (1972) The cupric ion as an inhibitor of photosynthetic electron transport in isolated chloroplasts. Plant Physiol **50:** 698–701

Chaney RL, Angle JS, McIntosh MS, Reeves RD, Li YM, Brewer EP, Chen KY, Roseberg RJ, Perner H, Synkowski EC, et al (2005) Using hyperaccumulator plants to phytoextract soil Ni and Cd. Z Naturforsch Sect C Biosci **60:** 190–198

Cobbett C, Goldsbrough P (2002) Phytochelatins and metallothioneins: roles in heavy metal detoxification and homeostasis. Annu Rev Plant Biol **53:** 159–182

Faucon MP, Ngoy Shutcha M, Meerts P (2007) Revisiting copper and cobalt concentrations in supposed hyperaccumulators from SC Africa: influence of washing and metal concentrations in soil. Plant Soil **301:** 29–36

Ferimazova N, Küpper H, Nedbal L, Trtílek M (2002) New insights into photosynthetic oscillations revealed by two-dimensional microscopic measurements of chlorophyll fluorescence kinetics in intact leaves and isolated protoplasts. Photochem Photobiol **76:** 501–508

Flynn KJ, Davidson K (1993) Predator-prey interactions between *Isochrysis galbana* and *Oxyrrhis marina*. I. Changes in particulate $\delta^{13}C$. J Plankton Res **15:** 455–463

Gallagher DL, Johnston KM, Dietrich AM (2001) Fate and transport of copper-based crop protectants in plasticulture runoff and the impact of sedimentation as a best management practice. Water Res **35:** 2984–2994

Gaudet T (1963) Marsilea vestita: conversion of the water form to the land form by darkness and by far-red light. Science **140:** 975–976

Genty B, Briantais J, Baker NR (1989) The relationship between the quantum yield of photosynthetic electron-transport and quenching of chlorophyll fluorescence. Biochim Biophys Acta **990:** 87–92

Hanson B, Garifullina GF, Lindblom SD, Wangeline A, Ackley A, Kramer K, Norton AP, Lawrence CB, Pilon-Smits EAH (2003) Selenium accumulation protects *Brassica juncea* from invertebrate herbivory and fungal infection. New Phytol **159:** 461–469

Jhee EM, Boyd RS, Eubanks MD (2005) Nickel hyperaccumulation as an elemental defense of *Streptanthus polygaloides* (Brassicaceae): influence of herbivore feeding mode. New Phytol **168:** 331–343

Korbas M, Marsa DF, Meyer-Klaucke W (2006) KEMP: a program script for automated biological x-ray absorption spectroscopy data reduction. Rev Sci Instrum **77:** 063105

Krämer U, Cotter-Howells JD, Charnock JM, Baker AJM, Smith JAC (1996) Free histidine as a metal chelator in plants that accumulate nickel. Nature **379:** 635–638

Küpper F, Küpper H, Spiller M (1996a) Eine aggressive Wasserpflanze aus Australien und Neuseeland: *Crassula helmsii* (Kirk) Cockayne (ein neuer Fund in Westfalen und eine Literaturübersicht). Florist Rundbr **30:** 24–29

Küpper H, Aravind P, Leitenmaier B, Trtílek M, Šetlík I (2007a) Cadmium-induced inhibition of photosynthesis and long-term acclimation to Cd-stress in the Cd hyperaccumulator *Thlaspi caerulescens*. New Phytol **175:** 655–674

Küpper H, Kroneck PMH (2005) Heavy metal uptake by plants and cyanobacteria. Met Ions Biol Syst **44:** 97–142

Küpper H, Küpper F, Spiller M (1996b) Environmental relevance of heavy metal substituted chlorophylls using the example of water plants. J Exp Bot **47:** 259–266

Küpper H, Küpper F, Spiller M (1998) In situ detection of heavy metal substituted chlorophylls in water plants. Photosynth Res **58:** 125–133

Küpper H, Lombi E, Zhao FJ, Wieshammer G, McGrath SP (2001) Cellular compartmentation of nickel in the hyperaccumulators *Alyssum lesbiacum, Alyssum bertolonii* and *Thlaspi goesingense*. J Exp Bot **52:** 2291–2300

Küpper H, Mijovilovich A, Meyer-Klaucke W, Kroneck PMH (2004) Tissue- and age-dependent differences in the complexation of cadmium and zinc in the Cd/Zn hyperaccumulator *Thlaspi caerulescens* (Ganges ecotype) revealed by x-ray absorption spectroscopy. Plant Physiol **134:** 748–757

Küpper H, Seibert S, Aravind P (2007b) A fast, sensitive and inexpensive alternative to analytical pigment HPLC: quantification of chlorophylls and carotenoids in crude extracts by fitting with Gauss-peak-spectra. Anal Chem **79:** 7611–7627

Küpper H, Šetlík I, Šetliková E, Ferimazova N, Spiller M, Küpper FC (2003) Copper-induced inhibition of photosynthesis: limiting steps of in vivo copper chlorophyll formation in *Scenedesmus quadricauda*. Funct Plant Biol **30:** 1187–1196

Küpper H, Šetlík I, Spiller M, Küpper FC, Prášil O (2002) Heavy metal-induced inhibition of photosynthesis: targets of in vivo heavy metal chlorophyll formation. J Phycol **38:** 429–441

Küpper H, Šetlík I, Trtilek M, Nedbal L (2000a) A microscope for two-dimensional measurements of *in vivo* chlorophyll fluorescence kinetics using pulsed measuring light, continuous actinic light and saturating flashes. Photosynthetica **38:** 553–570

Küpper H, Spiller M, Küpper F (2000b) Photometric method for the quantification of chlorophylls and their derivatives in complex mixtures: fitting with Gauss-peak-spectra. Anal Biochem **286:** 247–256

Küpper H, Zhao FJ, McGrath SP (1999) Cellular compartmentation of zinc

in leaves of the hyperaccumulator *Thlaspi caerulescens*. Plant Physiol **119:** 305–311

Lanaras T, Moustakas M, Symeonidis L, Diamantoglou S, Karataglis S (1993) Plant metal content, growth responses and some photosynthetic measurements on field-cultivated wheat growing on ore bodies enriched in Cu. Physiol Plant **88:** 307–314

Lane TW, Morel FMM (2000) A biological function for cadmium in marine diatoms. Proc Natl Acad Sci USA **97:** 4627–4631

Lidon FC, Ramalho JC, Henriques FS (1993) Copper inhibition of rice photosynthesis. J Plant Physiol **142:** 12–17

Martens SN, Boyd RS (1994) The ecological significance of nickel hyperaccumulation: a plant chemical defense. Oecologia **98:** 379–384

McGrath SP, Zhao FJ (2003) Phytoextraction of metals and metalloids from contaminated soils. Curr Opin Biotechnol **14:** 277–282

Mijovilovich A, Leitenmaier B, Meyer-Klaucke W, Kroneck PMH, Götz B, Küpper H (2009) Complexation and toxicity of copper in higher plants. II. Different mechanisms for copper versus cadmium detoxification in the copper-sensitive cadmium/zinc hyperaccumulator *Thlaspi caerulescens* (Ganges ecotype). Plant Physiol **151:** 715–731

Miwa Y, Mizuno T, Tsuchida K, Taga T, Iwata Y (1999) Experimental charge density and electrostatic potential in nicotinamide. Acta Crystallogr Sect B Struct Sci **55:** 78–84

Newman JR, Raven JA (1995) Photosynthetic carbon assimilation by *Crassula helmsii*. Oecologia **101:** 494–499

Ouzounidou G (1996) The use of photoacoustic spectroscopy in assessing leaf photosynthesis under copper stress: correlation of energy storage to photosystem II fluorescence parameters and redox change of P_{700}. Plant Sci **113:** 229–237

Ouzounidou G, Moustakas M, Lannoye R (1995) Chlorophyll fluorescence and photoacoustic characteristics in relationship to changes in chlorophyll and Ca^{2+} content of a Cu-tolerant Silene compacta ecotype under Cu treatment. Physiol Plant **93:** 551–557

Ouzounidou G, Moustakas M, Strasser RJ (1997) Sites of action of copper in the photosynthetic apparatus of maize leaves: kinetic analysis of chlorophyll fluorescence, oxygen evolution, absorption changes and thermal dissipation as monitored by photoacoustic signals. Aust J Plant Physiol **24:** 81–90

Pettifer RF, Hermes C (1985) Absolute energy calibration of x-ray radiation from synchrotron sources. J Appl Cryst **18:** 404–412

Pollard AJ, Powell KD, Harper FA, Smith JAC (2002) The genetic basis of metal hyperaccumulation in plants. Crit Rev Plant Sci **21:** 539–566

Prasad MNV, Hagemeyer J, editors (1999) Heavy Metal Stress in Plants: From Molecules to Ecosystems. Springer, Berlin

Rehr JJ, Albers RC (1990) Scattering-matrix formulation of curved-wave multiple-scattering theory: application to x-ray-absorption fine structure. Phys Rev B Condens Matter **41:** 8139–8149

Rocchetta I, Küpper H (2009) Chromium and copper induced inhibition of photosynthesis in Euglena gracilis analysed on the single-cell level by fluorescence kinetic microscopy. New Phytol **182:** 405–420

Sagner S, Kneer R, Wanner G, Cosson JP, Deus-Neumann B, Zenk MH (1998) Hyperaccumulation, complexation and distribution of nickel in Sebertia acuminata. Phytochemistry **47:** 339–347

Salt DE, Prince RC, Baker AJM, Raskin I, Pickering IJ (1999) Zinc ligands in the metal hyperaccumulator *Thlaspi caerulescens* as determined using x-ray absorption spectroscopy. Environ Sci Technol **33:** 712–717

Sanger JE (1971) Quantitative investigations of leaf pigments from their inception in buds through autumn coloration to decomposition of falling leaves. Ecology **52:** 1075–1089

Sarret G, Saumitou-Laprade P, Bert V, Proux O, Hazemann JL, Traverse A, Marcus MA, Manceau A (2002) Forms of zinc accumulated in the hyperaccumulator *Arabidopsis halleri*. Plant Physiol **130:** 1815–1826

Shen ZG, Zhao FJ, McGrath SP (1997) Uptake and transport of zinc in the hyperaccumulator *Thlaspi caerulescens* and the non-hyperaccumulator *Thlaspi ochroleucum*. Plant Cell Environ **20:** 898–906

Tomic S, Searle BG, Wander A, Harrison NM, Dent AJ, Mosselmans JFW, Inglesfield JE (2005) New Tools for the Analysis of EXAFS: The DL EXCURV Package. CCLRC Technical Report DL-TR-2005-001. Council for the Central Laboratory of the Research Councils, Swindon, UK

Walker DJ, Bernal MP (2004) The effects of copper and lead on growth and zinc accumulation of *Thlaspi caerulescens* J. and C. Presl: implications for phytoremediation of contaminated soils. Water Air Soil Pollut **151:** 361–372

Wang J, Zhao FJ, Meharg AA, Raab A, Feldmann J, McGrath SP (2002) Mechanisms of arsenic hyperaccumulation in *Pteris vittata*: uptake kinetics, interactions with phosphate, and arsenic speciation. Plant Physiol **130:** 1552–1561

Webb SM, Gaillard JF, Ma LQ, Tu C (2003) XAS speciation of arsenic in a hyper-accumulating fern. Environ Sci Technol **37:** 754–760

Wolf FT (1956) Changes in chlorophyll a and b in autumn leaves. Am J Bot **43:** 714–718

Zhao F, McGrath SP, Crosland AR (1994) Comparison of three wet digestion methods for the determination of plant sulphur by inductively coupled plasma atomic emission spectrometry (ICP-AES). Commun Soil Sci Plant Anal **25:** 407–418

Zhao FJ, Wang JR, Barker JHA, Schat H, Bleeker PM, McGrath SP (2003) The role of phytochelatins in arsenic tolerance in the hyperaccumulator Pteris vittata. New Phytol **159:** 403–410